Scattered-Light Intensity Fluctuations in Diastolic Rat Cardiac Muscle Caused by Spontaneous Ca^{++}-dependent Cellular Mechanical Oscillations

MICHAEL D. STERN, ARTHUR A. KORT, GOPAL M. BHATNAGAR, and EDWARD G. LAKATTA

From the Cardiovascular Section, Gerontology Research Center, National Institute on Aging, National Institutes of Health, Bethesda, Maryland 20205, and The Johns Hopkins Medical Institutions, Baltimore, Maryland 21224

ABSTRACT Laser light scattered by nonstimulated rat cardiac muscle bathed in physiological saline containing a $[Ca^{++}]$ of 0.4–2.5 mM displays scattered-light intensity fluctuations (SLIF); the frequencies of both SLIF and resting force are Ca^{++} dependent. Direct inspection of these muscles by phase-contrast microscopy under incoherent illumination revealed the presence of spontaneous asynchronous cellular motions that are also Ca^{++} dependent. The physical properties of the scattered light are compatible with the hypothesis that SLIF are due to the diastolic motion, except for the dependence on scattering angle, which may be perturbed because the muscles are optically thick. To determine whether diastolic SLIF and motion are an intrinsic property of activated myofilaments, photon-counting autocorrelation of the scattered light was performed both in rat right-ventricular papillary muscles skinned with the detergent Triton X-100 (1%) and in muscles with intact membranes under conditions that alter cellular Ca^{++} fluxes. In skinned muscles activated over a range of Ca^{++} from threshold to maximum force production, neither SLIF nor asynchronous motion was observed when Ca^{++} was buffered to constant values. In intact muscles the frequency of SLIF and the amplitude of diastolic motion were (*a*) markedly increased by substituting K^+ or Li^+ for Na^+ in the bath; (*b*) not altered by verapamil (1 μM); and (*c*) reversibly abolished by caffeine ($\geq$10 mM). These properties are exactly those of mechanical oscillations that have been observed in isolated cardiac cell fragments, which are the result Ca^{++} oscillations caused by Ca^{++} release from the sarcoplasmic reticulum (SR). We infer that mechanical oscillations caused by spontaneous Ca^{++}-induced Ca^{++} release from the SR occur in intact nonstimulated cardiac muscle even in the absence of Ca^{++} overload and are the principle cause of SLIF, and that myoplasmic $[Ca^{++}]$ in "resting" muscle is not in a microscopic steady state.

Address reprint requests to Dr. Edward G. Lakatta, Cardiovascular Section, Gerontology Research Center, National Institute on Aging, Baltimore, MD 21224.

J. GEN. PHYSIOL. © The Rockefeller University Press · 0022-1295/83/07/0119/35 $1.00 119
Volume 82 July 1983 119–153

INTRODUCTION

Intensity fluctuations in coherent light scattered from complex structures are a well-known phenomenon. Light scattered from a complex object consists of a superposition of many wavefronts traveling by optical paths of different lengths. This results, if the scattering object is stationary (at the microscopic level), in random interference fringes visible to the eye as a speckle pattern. If some microscopic process within the object causes the optical pathlengths to vary with time, the random interference pattern will fluctuate, manifested by a scintillation of the speckle pattern (if the fluctuation is slow enough to be resolved by the eye) and by fluctuation of the scattered-light intensity measured at a single point in the scattering pattern. Processes that can cause this effect are of two kinds: microscopic motion of the light scatterers in the object or fluctuation of the refractive index of structures in the object.

Lappe and Lakatta (1980) showed that intensity fluctuations are present in laser light scattered from living isolated rat papillary muscles bathed in physiologic saline containing a $[Ca^{++}]$ of 0.4–2.5 mM in the unstimulated state, when the muscles are apparently quiescent. By autocorrelating the intensity of these fluctuations as a function of time, the average frequency ($f_{1/2}$) was defined as the reciprocal of the time for 50% decay of the autocorrelation function (see below). It was observed that (*a*) $f_{1/2}$ depended directly on the concentration of Ca^{++} bathing the muscle, $[Ca^{++}]_e$, and in the absence of $[Ca^{++}]_e$ (buffered with EGTA) the fluctuations disappeared; (*b*) $f_{1/2}$ varied with $[Ca^{++}]_i$ when the latter was increased by application of ouabain, by depolarizing the sarcolemma with KCl, or by lowering $[Na^+]_e$, which indicates that the level of $[Ca^{++}]_i$ is probably of primary importance in mediating the Ca^{++} effect on light-scattering fluctuations. It was also observed that a fraction of the resting tension in non–Ca^{++}-overloaded rat papillary muscles was Ca^{++} dependent, and that the Ca^{++}-dependent resting force correlated closely and usually linearly with $f_{1/2}$ during all the above manipulations. These results were interpreted as showing that scattered-light intensity fluctuations (henceforth SLIF) are due to an active phenomenon that probably involves Ca^{++} activation of myofilaments even in the resting or diastolic state.

In the present study three parallel approaches were taken to determine the mechanism of SLIF in heart muscle. (*a*) Papillary muscles were examined by phase-contrast microscopy under coherent illumination in order to detect the presence of SLIF manifested as scintillation of the speckle pattern produced in the image, and under incoherent illumination to see whether motion could be observed and whether this varied with SLIF in states in which SLIF are known to vary. (*b*) Photon-counting autocorrelation of the scattered light was performed, the fluctuation spectrum was examined as a function of the scattering angle, and the photon statistics of the scattered light were studied. These data permit inferences as to the presence of longitudinal motion of scatterers and the

fraction of light that has been scattered by independently fluctuating systems. (*c*) The effect on SLIF of interventions designed to dissect physiologically the fluctuation process was examined. These included "chemical skinning" of the muscle and direct activation the myofilaments with steady levels of free Ca^{++}; blocking electrical events at the sarcolemma by removing $[Na^+]_e$, depolarizing with high levels of $[K^+]_e$, or blocking slow channels with verapamil; blocking sarcoplasmic reticulum (SR) Ca^{++} transport by application of caffeine; and combinations of these interventions.

As described below, these studies showed that SLIF are correlated with the presence of random, asynchronous, wavelike mechanical oscillations throughout the diastolic muscle, which under microscopic examination appear to be partially periodic at any one location within the muscle. Because of multiple scattering effects, as well as the absence of a quantitative description of the mechanical oscillations, it is not possible to calculate the spectrum of scattered-light fluctuations quantitatively. We show, however, by examining a model of first-order scattering from an array of scatterers in partially periodic asynchronous motion, that this model can explain many of the qualitative features of the correlation functions, provided that Ca^{++} and caffeine are assumed to act on the mechanical amplitude and frequency of the mechanical oscillations in prescribed ways. These assumptions turn out to bear a close resemblance to the properties of oscillations that others have studied in single cardiac cells and cell fragments and which are believed to be due to spontaneous Ca^{++}-induced Ca^{++} release from the SR. The occurrence of asynchronous cellular motion in diastole explains, at least in part, the previously observed Ca^{++}-dependent resting tone. By examining a highly idealized model of independent asynchronous cellular oscillators, we show that temporal synchronization of cells (e.g., by a depolarizing stimulus) could produce oscillatory force transients, i.e., a twitch followed by aftercontractions, similar to those aftercontractions that are routinely observed in rat papillary muscles after stimulation.

METHODS

Muscle Preparation

Wistar rats weighing 300–500 g were killed by cervical dislocation and the hearts were placed in oxygenated Krebs-Ringer bicarbonate or HEPES-buffered solution (Lakatta and Lappe, 1981) containing a $[Ca^{++}]$ of 1 mM, a $[K^+]$ of 4.2 mM, and a $[Mg^{2+}]$ of 1.0 mM. Right-ventricular papillary muscles (100–400 μM diam) were dissected and mounted between stainless-steel clips attached to a force transducer (UC-2; Statham Inc., Oxnard, CA) and perfused with Krebs solution at 28°C, either in a 3-ml light-scattering chamber or in a 5-ml plastic petri dish mounted on the stage of an inverted microscope (Leitz Diavert; E. Leitz, Inc., Rockleigh, NJ). Muscles were field-stimulated (SD9; Grass Instrument Co., Quincy, MA) at 24 min^{-1} with platinum wire electrodes. After the developed

force stabilized, muscles were stretched to the peak of the length-developed force curve (sarcomere length 2.0–2.2 μm in those muscles thin enough to show a diffraction pattern) and equilibrated further for 2 h.

Microscopy

Muscles mounted as described were positioned so that the free edge of the muscle could be examined by phase-contrast microscopy, using a 25-magnification phase-contrast objective and a 12.5-magnification eyepiece. The image was photographed using a 16-mm H16 motion picture camera (Bolex, Zurich, Switzerland) at 18 frames/s. Two alternative sources of illumination were used. In each scene the muscle was first photographed while illuminated from above by incoherent tungsten light through a green filter, using the normal illumination optics of the microscope. The same scene was then photographed with the muscle directly illuminated by the beam of a 5-mW He-Ne laser (632.8 nm; 147, Spectra-Physics Inc., Mountain View, CA) directed on the muscle from above, through the free surface of the perfusion fluid, from an angle of 20° above the horizontal. Under coherent illumination, the outlines of the muscle were visible, but the internal structure was dominated by the coarse speckle pattern formed through the microscope and camera optics. When living muscle was examined in the absence of Ca^{++}, a stationary speckle pattern was observed; in the presence of Ca^{++}, the speckle pattern appeared to be in a constant state of random "motion" with bright speckles and dark alternating in rapid sequence at any one location. This effect results from the intensity fluctuations, which are present at each point in the scattering field, but are independent at different points separated by more than a "coherence area" (Saleh, 1978), creating the illusion of chaotic motion. Muscles were photographed under the following conditions: immediately after mounting, after equilibration for 2 h, after addition of 10 mM caffeine to the perfusion medium, after removal of caffeine, during the force transient produced by removing $[Na^+]_e$, and after the muscle had been "chemically skinned" in the microscope chamber by the protocol described below.

Light-Scattering Studies

For formal light-scattering studies the muscle was perfused in a 3-ml chamber with sides made from glass microscope slides as described in Lappe and Lakatta (1981). The muscle was illuminated by a beam of He-Ne laser light, collimated by passage through a 1-mm pinhole and polarized horizontally (in the plane containing the long axis of the muscle), directed at right angles to the long axis. The laser intensity was adjusted by rotating a half-wave plate between the laser (linearly polarized) and the horizontal polarizing filter. Light scattered in the horizontal plane at an adjustable angle was collected through an adjustable pinhole (75–400 μm) located 20 cm from the muscle and focused by a convex lens on a second aperture of 600 μm diam at the entrance to a photomultiplier tube (Fig. 1). The arrangement was designed so that the effective object was a circular region of the illuminated muscle defined by the 600-μm aperture in the image plane (and therefore constant in size), while the adjustable pinhole determined the number of coherence areas (Saleh, 1978) from which light was collected. A linear polarizer was placed in the collection pathway to sample scattered light of a single (usually horizontal) polarization. Light was collected on a photon-counting photomultiplier tube (RR51; Malverne Instruments, Worcester, England) and the counts were analzyed by a digital autocorrelator

(K7025; Malverne Instruments). Correlation functions were computed by digitally averaging the product $n(t)\ n_p(t + \Delta t)$ where $n(t)$ is the number of photons counted during a sample period at time t, and $n_p(t + \Delta t)$ is the photon count at time $(t + \Delta t)$ prescaled by a power of 2 so as to be expressible within the four-bit range of the second channel of the correlator. (It can be shown [Saleh, 1978] that the expectation value of this "single prescale" autocorrelation function is directly proportional to the full digital correlation function $n(t)\ n\ (t + \Delta t)$, presuming only that the light forms a stationary random process.) The correlator was controlled by a desk-top computer (9825A; Hewlett-Packard Co., Palo Alto, CA), which automatically selected averaging times and prescale levels so as to obtain a precision of 5% in accordance with equations in Saleh (1978). The

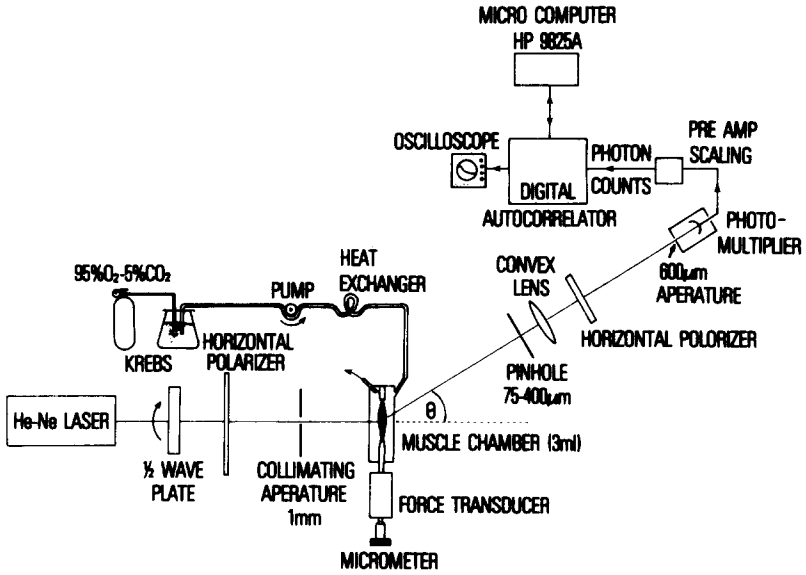

FIGURE 1. Block diagram of apparatus for formal quasi-elastic light-scattering studies of rat papillary muscles. The scattering angle and the size of the pinhole are adjustable. The convex lens is positioned so as to form a real image of the muscle on the 600-μm aperture of the photomultiplier housing.

correlation functions were normalized by the HP-9825A by dividing by the theoretical asymptotic value of the correlation function $\langle n \rangle^2$ computed from the rate of photon counting averaged over the entire data-collection interval (typically 1,000 times the largest value of Δt for which the autocorrelation function itself was computed). The values of Δt and total averaging times were chosen iteratively so as to give nominal 5% precision to the estimates of $f_{1/2}$ and amplitude. Fig. 2 shows a typical normalized autocorrelation function of light scattered at 30° from a resting muscle. As shown, $f_{1/2}$ is defined as $\frac{1}{2\pi\ t_{1/2}}$, where $t_{1/2}$ is the time for the autocorrelation function to decay 50% of the way to baseline. The autocorrelation amplitude, defined as $g(0) - 1$, was also computed on-line; it is a

measure of the degree of intensity modulation of the light, being equal to (variance of intensity)/(mean intensity)^2. In cases where $f_{½}$ is small, averaging times of several minutes resulted. In such cases, the presence of very long period fluctuations (such as would result from slow secular stretching of the illuminated muscle segment) would result in higher values of amplitude and lower estimates of $f_{½}$ than would appear from inspection of the autocorrelation function. Because it cannot be determined what fraction of long period fluctuations is "artifactual," it is difficult to define the true accuracy of the measurements in cases where the autocorrelation decay is not complete within several seconds, except as an upper limit on the amplitude and a lower limit on $f_{½}$.

Chemical Skinning

To determine whether scattered-light fluctuations, as observed either under the microscope or in the autocorrelation experiments, are produced when myofila-

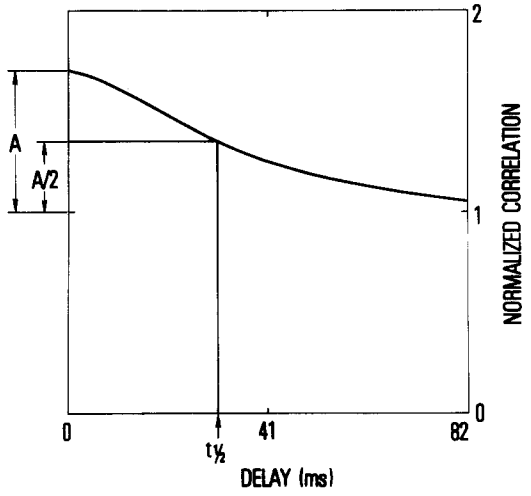

FIGURE 2. Normalized photon-count autocorrelation function of laser light scattered at 30° from a papillary muscle giving an $f_{½}$ of 5.1 Hz. The normalized autocorrelation function is defined as $\langle n(t)n(t + \Delta t)\rangle/\langle n(t)\rangle^2$ (the prescaled correlation was actually computed and multiplied by the prescale fraction, giving the same result [Saleh, 1978]). The definition of the autocorrelation amplitude, A, and the half-decay time, $t_{½}$, from which $f_{½}$ is determined, are shown.

ments are directly activated by constant levels of free Ca^{++}, muscles were chemically skinned by the following protocol designed to ensure destruction of membraneous organelles, thereby permitting control of myoplasmic [Ca^{++}]. After muscles were mounted and equilibrated and $f_{½}$ was measured, the muscles were cooled to 22°C (which had little effect on $f_{½}$) and then perfused for 30 min with Krebs-Ringer containing 5 mM EGTA and no Ca^{++}. Membranes were then disrupted by a 30-min perfusion with Triton X-100 (1%) dissolved in a relaxing solution containing 100 mM KCl, 7 mM $MgCl_2$, 5 mM ATP, 3 mM EGTA, 7.5 mM creatine phosphate, and 0.05 mg/ml creatine phosphokinase, and buffered to pH 7.0 with 25 mM imidazole. Detergent was removed by washing with fresh

relaxing solution, after which stepwise activation was produced by perfusion with solutions made up to a known pCa from relaxing solution using the computer programs of Fabiato and Fabiato (1979). Activation curves were repeated two or more times in each muscle, and at the end of the experiment, ATP was removed from the relaxing solution to demonstrate production of rigor force as evidence for completeness of skinning (Reuben and Wood, 1979).

Intact Muscle Studies

Intact muscles were perfused with graded concentrations of caffeine (0.1–20 mM) dissolved in the Krebs perfusate buffered to pH 7.4 and made up to constant osmotic strength with sucrose. In other studies, Na^+ was replaced by Li^+ in the bath and the resulting transients of force and $f_{1/4}$ were measured. In other muscles, depolarization of the sarcolemma was produced by replacing NaCl with equimolar KCl and the resulting force transients and $f_{1/4}$ were monitored for 30 min. The effect of verapamil was studied by the following protocol. Muscles were equilibrated and developed force was measured. Stimulation was then stopped, and the muscles were perfused for 30 min with *dl*-verapamil (1 μM) dissolved in Krebs, while $f_{1/4}$ was measured intermittently. After this, the muscles were again stimulated, with the reduction of developed force taken as evidence of slow channel blockade. Each of these protocols were repeated in additional muscles, which were studied under the microscope using both coherent and incoherent illumination as described above.

RESULTS

Direct Microscopic Studies

The free edge of intact papillary muscles was examined at a magnification of 312 under incoherent illumination. At this magnification, internal structures are resolved as a jumble of detail, especially away from the edge, where the muscle is optically thick. Sarcomere structure was faintly visible and observed only in some preparations at this magnification. In muscles examined shortly after mounting in perfusate [Ca^{++}] of 1 mM, a continuous, chaotic "squirming" motion was observed, which gradually diminished in amplitude with time, becoming quite subtle after several hours. In muscles equilibrated in perfusate containing 3 mM Ca^{++}, the motion continued indefinitely at an amplitude that was conspicuous at the magnification employed. Description of the motion is necessarily subjective; it appeared to consist of random waves of contraction proceeding in both directions along the muscle, asynchronous throughout the length. There was an apparent preferred direction of these waves. Individual waves appeared to be roughly 10–30 μm in length and could be seen along the edge of the muscle as bulges that died out and reformed as they traveled, resembling water waves rolling onto a beach. Within the body of the muscle, the waves appeared under phase contrast as dark bands within which longitudinal to-and-fro motion of subcellular structures was seen. Overall, the entire muscle appeared to be in a state of random motion; however, examination of small regions showed a tendency toward local periodicity of the motion, the estimated frequencies

of which were ~1–2 Hz, although this varied from one point on the muscle to another. The excursion of any one point in the muscle appeared to be ~1–10 μm under these conditions. When the muscle was Ca^{++} loaded by replacing Na^+ in the medium with Li^+, the squirming motions became larger, somewhat faster, and possibly more disordered. The overall impression then was of a "washing machine" with prominent periodic oscillation of small domains of the muscle, completely asynchronous from one region to another even within the 200-μm length of the microscope field. The predominance of unidirectional wave travel was not apparent under these conditions.

Under coherent (laser) illumination, the internal detail of the muscle was completely overshadowed by the speckle interference pattern. In the living muscle, this speckle pattern was in a turmoil of chaotic motion, with bright and dark speckles changing places rapidly as intensity fluctuated at different points of the field. The apparent speed of speckle motion varied with the Ca^{++} bathing the muscle; during low-Na^+ contracture, the "motion" began to blur as the frequency of intensity fluctuations approached the flicker-fusion frequency of the eye. In the absence of Ca^{++}, or when the muscle was subjected to prolonged deprivation of oxygen and substrate, or when membranes were destroyed with Triton X-100, the squirming motion seen under incoherent light was abolished. Under the same conditions, the speckle pattern seen under coherent illumination was entirely stationary.

Coherent Light-Scattering Studies

Fig. 3 shows the raw (un-normalized) photon-count autocorrelation functions for a muscle in several concentrations of Ca^{++}. As can be seen, the slope of the autocorrelation decay increased with $[Ca^{++}]_e$, as previously described using analog correlation techniques (Lappe and Lakatta, 1980; Lakatta and Lappe, 1981). Fig. 4 shows the effect of variation of $[Ca^{++}]_e$ on $f_{1/2}$ derived from these correlation functions. By using digital photon-counting correlation techniques, it was possible to recover the absolute amplitude of the correlation decay, which has been plotted on the same figure. At low levels of $[Ca^{++}]_e$, as $f_{1/2}$ decreased (Fig. 4), the correlation amplitude decreased from the asymptotic value seen at higher $[Ca^{++}]_e$. Roughly speaking, the amplitude is a measure of the fraction of the light reaching the detector that is intensity modulated; more precisely, it is related to the photon statistics of the scattered light.

Coherent light scattered by a stationary object has constant intensity; according to quantum theory, the number of photons detected in a fixed sampling period fluctuates randomly with a Poisson distribution. The correlation amplitude is so defined that it is zero for constant-intensity (Poisson) light. Light that is the superposition of a large number of wavefronts of random and independently varying phases has a circular Gaussian electromagnetic field distribution; in this case, the number of photons in a fixed sampling interval (short compared with the correlation

time), in the limit where the detector is small compared with a coherence area (Saleh, 1978), has an exponential distribution. Exponentially distributed light has a correlation amplitude of 1.0. Light that is a mixture of coherent light scattered from stationary structures and Gaussian light scattered from a large number of fluctuating structures will have an intermediate distribution, with intermediate values of amplitude. Other effects that may reduce the amplitude include the finite size of the detector area, the presence of only a small number of independently fluctuating scatterers in the illumination volume, or the limitation of the

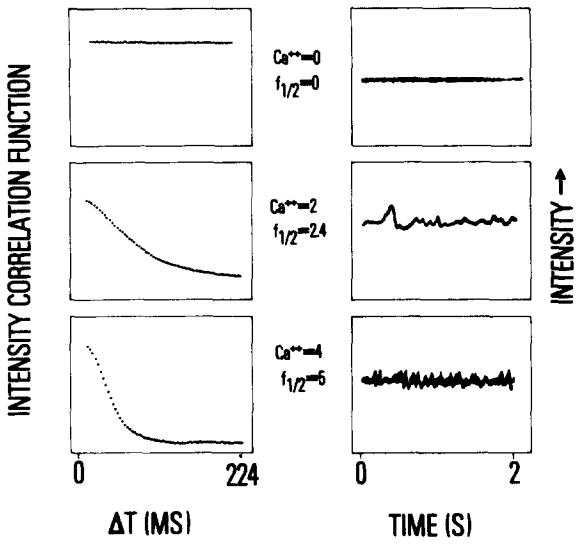

FIGURE 3. Raw (un-normalized) photon-count autocorrelation functions of light scattered at 30° from one muscle at three concentrations of bathing Ca^{++}. The baselines have been displaced to suppress the constant baseline $\langle n(t)\rangle^2$ caused by the mean intensity of the light. The rapidity of correlation decay clearly varies with Ca^{++}, as reflected in the level of $f_{1/2}$ calculated from these correlation functions. The right-hand panels show the fluctuating component of intensity in the time domain, which illustrates the relationship of the correlation function to the frequency of intensity fluctuations.

fluctuation of optical pathlength of any one scatterer to values smaller than a wavelength. The latter situation pertains, for example, when the scatterers are all in motion but are constrained to move within a fraction of a wavelength of light from their original positions.

To quantitate photon statistics of light scattered from rat papillary muscle, the probability distribution for the arrival of n photons during any 2-ms sample window (short compared with $t_{1/2}$) within a 2-min averaging period (long compared with coherence time) was measured (Fig. 5). For comparison, exponential and Poisson distributions are plotted on the same figure, showing that the data are well fit by the exponential

distribution in this case, where the muscle was equilibrated in a $[Ca^{++}]_e$ of 2 mM and measurements were made through the smallest (75 μm) pinhole to sample a fraction of a coherence area. Use of larger pinholes resulted in deviation from the exponential distribution at low photon numbers, as expected. These results are compatible with (though not sufficient to prove rigorously) the presence of Gaussian statistics in the scattered light at moderate and upper levels of $[Ca^{++}]_e$. However, the results of direct microscopy showed that all structures in the tissue undergo displacements greater than a wavelength of light under these conditions and that the size of the co-moving region appeared to be much smaller than the illuminated area of the muscle in the scattering apparatus. These conditions would be expected to give rise to field statistics that were approxi-

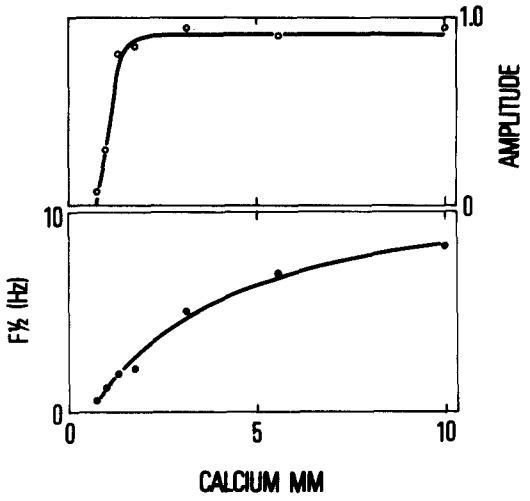

FIGURE 4. The effect of variation of bathing $[Ca^{++}]$ on $f_{½}$ and correlation amplitude of light scattered at 30° from a typical rat papillary muscle.

mately Gaussian. Decreasing the illuminated area of the muscle to 200 μm did not result in detectable changes in photon statistics.

The simplest explanation of the decrease in correlation amplitude in low $[Ca^{++}]_e$ (Fig. 4) would be that the fluctuating displacement of scatterers becomes appreciably smaller than the wavelength of light. The mechanical amplitude of the tissue motion seen during microscopy with incoherent illumination certainly varied with Ca^{++}; since fluctuations in the laser speckle pattern were still visible when the motion was too subtle to be defined with certainty under incoherent light, it is difficult to exclude the possibility that, at low levels of Ca^{++}, regions within the muscle are entirely stationary, which would have a similar effect on the photon statistics as that caused by a uniform decline in the displacement amplitude of all regions of the muscle.

The variation of $f_{½}$ and correlation amplitude with scattering angle in

the horizontal plane is shown in Figs. 6 and 7. Fig. 6*A* shows the mean and standard deviation of $f_{1/2}$ from five different muscles, normalized to unity for each muscle at an angle of 30°. The trend toward a linear increase in $f_{1/2}$ with sine θ is evident and continues to higher values of θ, which we have studied in other muscles. The "bump" in the curve at angles of 24–27° appears to be a real phenomenon, insofar as it is seen in most individual muscles. This phenomenon is probably related in some way to sarcomere diffraction effects, although the exact relationship is not clear, since the diffraction maxima occurred at 18° and 38° in these

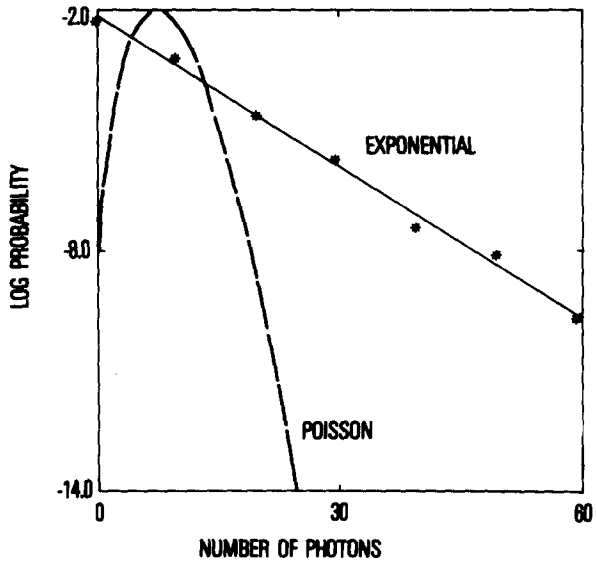

FIGURE 5. *A posteriori*-measured photon-count probability distribution of laser light scattered at 30° from a rat papillary muscle. The ordinate shows the log probability of detecting n photons during any 2-ms interval in a 2-min averaging period, as a function of n. For comparison are shown an exponential distribution (straight line) expected for circular Gaussian light and a Poisson distribution (dashed curve) expected for steady coherent light having the same mean intensity.

muscles (which were carefully selected to have prominent diffraction patterns).

It is of importance that $f_{1/2}$ extrapolated to a scattering angle of zero does not go to zero. As discussed in Bonner and Carlson (1975) and Haskell and Carlson (1981), for systems in which fluctuations are caused by longitudinal motion of scatterers, $f_{1/2}$ will be a function of the sine of the scattering angle that vanishes at zero angle. The exact variation is related to the statistical nature of the motion, being linear in cases where the motion proceeds at constant velocity for distances longer than the wavelength of light, quadratic for unidirectional Brownian motion, etc.

Accordingly, the presence of significant fluctuation frequency at zero scattering angle might be taken as evidence that fluctuations of refractive index rather than motion were responsible for most of the fluctuation. Such a conclusion is only warranted if the muscle can be considered optically thin, i.e., manifesting little or no multiple scattering and not showing "deep-phase screen" effects, which occur when the direct optical pathlength through the muscle varies by more than a wavelength from point to point. Cardiac muscle consists of a variety of microscopic structures (e.g., 40% mitochondria, SR, myofilaments, etc.) arranged irregu-

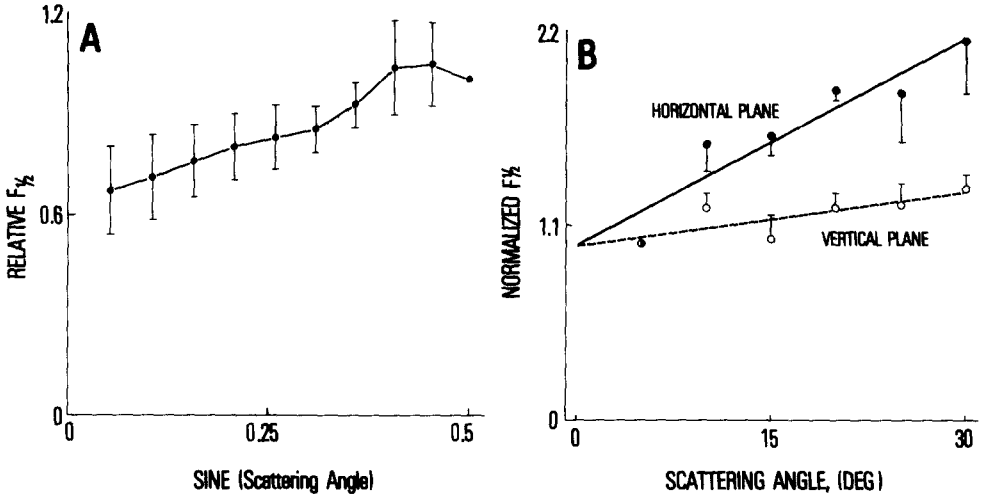

FIGURE 6. (*A*) Variation of $f_{½}$ with the sine of the scattering angle in the horizontal plane for five papillary muscles. The curve represents the mean of the curves obtained by normalizing the $f_{½}$ of each muscle to unity at 30° scattering angle. The error bars represent the standard deviation among muscles. (*B*) Variation of normalized $f_{½}$ with scattering angle in the horizontal (longitudinal) and vertical scattering planes averaged in three additional muscles. $f_{½}$ was normalized to the value at 5° in each muscle, and the bars represent the SEM. The points were fit by linear regressions with a slope of 0.039 in the horizonal plane and 0.010 in the vertical plane; $P < 0.008$.

larly, so it would not be surprising if a muscle many cells deep manifested deep-phase screen effects. This is confirmed by the fact that only at the thinnest edge of the muscles was it possible to resolve subcellular structures by phase-contrast microscopy. These muscles appeared translucent rather than transparent under the dissecting microscope, and they obscured most of the direct laser beam illuminating them. Furthermore, microscopy of the edge of actively fluctuating muscles showed that individual contractile waves produce moving "bulges" several microns or more in height on the surface of the muscle. The geometrical thickness of the muscle therefore fluctuates by this much, so it is not unlikely that

the direct (zero angle) optical thickness fluctuates by a significant fraction of a wavelength. The resulting deep-phase screen effect would produce significant intensity fluctuations even at very low scattering angles.

Fig. 6*B* shows the variation of $f_{1/4}$ in three additional muscles in which angle scans were performed both in the horizontal and vertical planes (i.e., the planes parallel and perpendicular to the muscle axis). The angular variation in the vertical plane is significantly less than that in the horizontal plane, as would be expected if the underlying motion is largely along the axis of the muscle.

Fig. 7 shows the variation of correlation amplitude with scattering angle

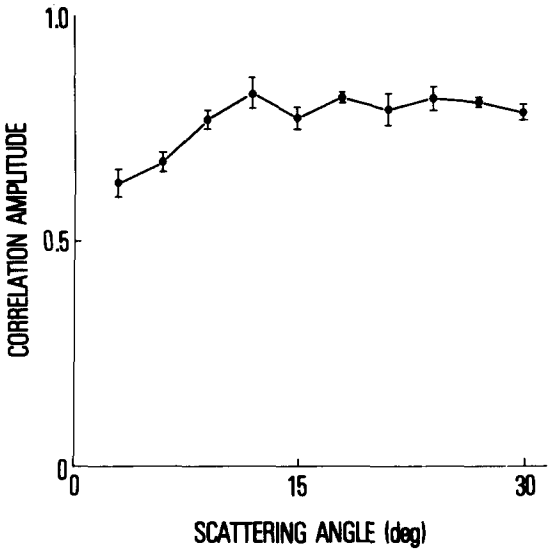

FIGURE 7. Scattering angle dependence of the autocorrelation amplitude (a pure number) averaged from muscles in Fig. 6*A*. Muscles chosen were thin enough to show good diffraction patterns, which all had the first-order peak at 18°. The error bars are the SEM. Light was collected through a 200-μm pinhole, which resulted in maximal amplitude of less than unity for Gaussian light.

for three muscles. The amplitude is essentially constant for scattering angles above 12° and is equal to the value at 30°, which, as discussed above, is compatible with Gaussian statistics (pinhole 200 μm in this case). Below 12° the amplitude falls off somewhat, but it does not approach zero, as would be expected for first-order scattering from a linear array of constrained moving scatterers. The reasons for this are presumably the same as discussed above for the low-angle behavior of $f_{1/2}$. There was no significant variation of amplitude with angle in the vertical plane in the muscles shown in Fig. 6*B*.

The fact that the amplitude does decrease somewhat at lower angles

suggests that zero-angle optical pathlength fluctuations are at most about one wavelength; however, similar results could occur if low-angle scattered light consisted of an admixture of unmodulated first-order scattering and intensity-modulated, multiply scattered light. The fact that the amplitude does not decrease on the diffraction peak at 18° at first seemed surprising, since these measurements were made before our microscopic studies of the motion. Amplitude might be expected to decrease at the peak because of the admixture of elastically scattered (coherent) light diffracted by the periodic sarcomere lattice. This has been shown to be the case in single skeletal muscle fibers by Haskell and Carlson (1981). However, cardiac muscle consists of a large number of short cells. The diffraction pattern is therefore a superposition of contributions from many short segments of periodic lattice whose relative phases are random since they are not in registry. This is confirmed by the fact that the diffraction peaks actually consist, when examined closely, of a fine, random speckle pattern on which the diffraction pattern is superimposed as a modulation envelope. Relatively gross, diastolic contractile waves of the sort that we have seen, whose "wavelength" is long compared with sarcomere spacing but short compared with the illuminating beam diameter, would have the effect of randomly shifting the phases of the different cellular sublattice contributions to the diffraction pattern, giving rise to Gaussian field statistics even at the diffraction peak. Measurements of photon statistics at the diffraction peak show a nearly exponential distribution except for fall-off in the first few bins, which indicates that only a small fraction of the light at the peak is in fact unmodulated in this preparation. It is of interest that at very high levels of $[Ca^{++}]_e$ the diffraction pattern itself is suppressed (Lakatta and Lappe, 1981), possibly because of short-range disorder of sarcomere lengths produced when the random waves of contraction are intense. It is indeed noteworthy that SLIF can be readily measured on thick muscles that show little or no diffraction pattern.

As described above, the random tissue motion seen under the microscope appears to be at least partially periodic on a local scale, with an estimated dominant period of the order of 1 Hz; any periodicity of the SLIF at this frequency would not have been observed in the correlation functions shown above, as they were calculated only to $\Delta t = 225$ ms. We therefore examined the autocorrelation function on a longer timebase (and at higher gain), searching for secondary peaks indicative of periodicity. As shown in Fig. 8, no such peaks were seen out to $\Delta t = 3$ s in the case of actively fluctuating muscles under normal levels of Ca^{++} loading. The reasons for this, and the conditions under which such peaks are seen, are discussed in the Appendix in the context of model calculations of scattering.

Chemical-skinning Studies

To determine whether the Ca^{++}-dependent SLIF and the tissue motions that appear to be associated with them are an intrinsic result of Ca^{++}

activation of myofilaments, muscles were chemically skinned as described above. These chemically skinned muscles were capable of reversible activation to produce ~75% of twitch force at micromolar levels of free Ca^{++}. Fig. 9 shows a force-pCa curve, obtained as an average from six muscles. The curves are quite reproducible within and among muscles, and resemble those obtained by others in "detergent-skinned" preparations (McClellan and Winegrad, 1978; Endo and Kitazawa, 1978) and mechanically skinned cardiac cells (Fabiato and Fabiato, 1975*a*). As shown in the upper panel of the figure, direct activation by Ca^{++} buffered to constant levels did not produce SLIF. The correlation function of scattered light was completely flat ($f_{1/2} = 0$) at all levels of activation. In these preparations, removal of ATP produced rigor force (again with $f_{1/2} = 0$) that was reversible if ATP was quickly replaced. Addition of caffeine did not produce contracture. These results are compatible with the assump-

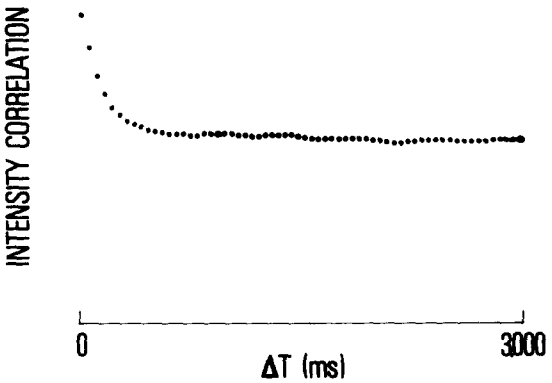

FIGURE 8. Long timebase autocorrelation function of light scattered at 30° from a papillary muscle in Ca^{++} of 2 mM. The timebase is 3 s and the gain has been increased to search for secondary correlation peaks, resulting in an overflow of the primary peak. The baseline has been suppressed.

tion that myofilaments were directly activated by constant levels of free Ca^{++}, with functional destruction of sarcolemma and SR.

When the same chemical-skinning procedure was carried out in the microscope chamber, the random diastolic motion disappeared after skinning, and the muscle appeared stationary both in relaxing solution and over the entire range of Ca^{++} activation. The speckle pattern of the skinned muscle under coherent illumination was stationary at all levels of activation.

Intact Muscle Studies

The above results indicate that SLIF and the random diastolic motion with which they appear to be associated are not an intrinsic property of myofilaments in a steady state of activation. However, fluctuating activation of the myofilaments, i.e., that caused by fluctuations of myoplasmic $[Ca^{++}]$ within the cell in diastole, could produce motion. To determine

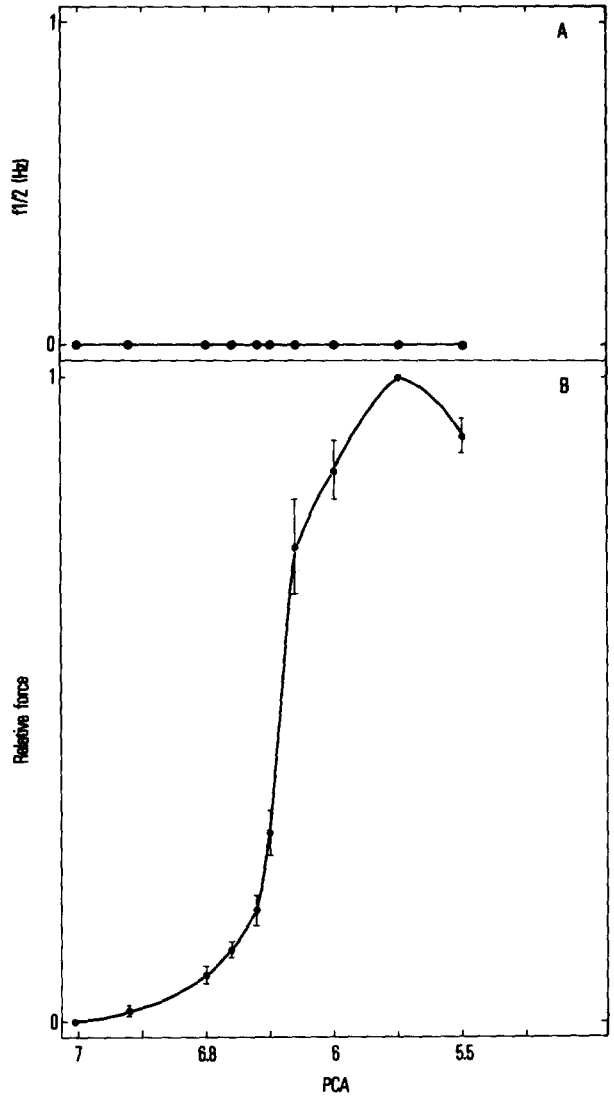

FIGURE 9. Force-pCa curve for the activation of detergent-skinned rat papillary muscles in contracture solutions Ca^{++}-buffered with 3 mM EGTA. The lower panel shows relative force produced (mean ± SEM, $n = 6$). The upper panel shows $f_{1/2}$, which was always zero (absent SLIF) at all levels of activation.

whether fluctuations of this sort generated by fluctuating sarcolemmal currents cause SLIF, muscles were exposed to conditions expected to block various types of sarcolemmal electrical processes, viz. $[Na^+]_e = 0$ to disable the Na^+ channels, $[K^+]_e = 144$ mM to depolarize the sarcolemma, or verapamil (1 μM) to block Ca^{++} channels. The results are shown in Fig. 10. Replacing the 144 mM Na^+ in Krebs solution by Li^+ (Fig. 10*A*) or K^+

(Fig. 10*B*) produced force transients that decayed within 30 min to a level of force equal to or greater than control. Under these conditions the muscle was electrically inexcitable. Scattered-light fluctuations were not abolished by these procedures; rather, $f_{1/2}$ increased with force during the

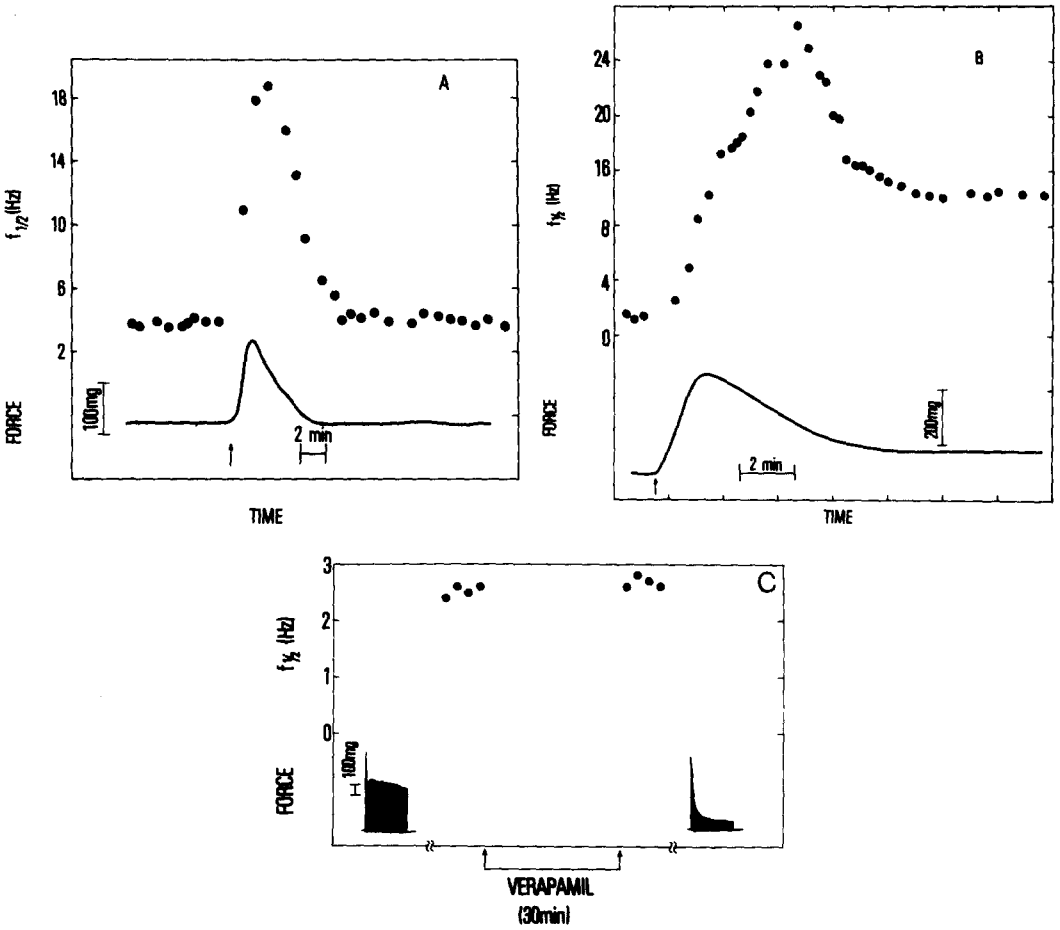

FIGURE 10. (*A*) Force transient (solid line) and $f_{1/2}$ (dots) from a rat papillary muscle in which $[Na^+]_e$ was replaced by Li^+ at the time shown by the arrow. (*B*) Similar force and $f_{1/2}$ transients produced by replacing $[Na^+]_e$ by K^+ in another muscle. (*C*) Measurements of $f_{1/2}$ before and after addition of verapamil 1 μM to the bath. Force tracings are shown for the muscle regularly stimulated 24 times/min before and after incubation with verapamil. The scattering angle was 30° in all cases.

transient, consistent with an effect of increased $[Ca^{++}]_i$ loading, and then stabilized at a steady level proportional to resting force. Fig. 10*C* shows that verapamil applied to resting muscle caused no change in $f_{1/2}$. Verapamil was applied while the muscle was resting in order to preclude the

possibility that it would alter $[Ca^{++}]_i$ by reducing the amount of Ca^{++} entering during an action potential. When the muscle was later stimulated in verapamil, there was in fact a rapid decline in developed force, indicative of verapamil's effect to block the slow inward Ca^{++} channel. We interpret the results of these three studies as evidence that known electrical processes at the sarcolemma are not directly required for the generation of SLIF. Table I summarizes the results of the experiments shown in Fig. 10, averaged over several muscles, which confirm the reproducibility of these phenomena.

Fluctuating activation of the myofilaments could be produced by uptake and release of Ca^{++} from intracellular stores. Caffeine is believed to act directly on SR, causing release of Ca^{++} and preventing its re-uptake (Endo, 1977). At levels below 20 mM it probably does not have significant effects on myofilaments, mitochondria, or resting membrane potential (Weber, 1968; Kimoto et al., 1974; Blayney et al., 1978). It has been

TABLE I

Interventions Attempting to Abolish or Reduce SLIF Caused by Sarcolemmal-mediated Ca^{++} Fluxes

	$f_{1/2}$ (Hz)		
	Control	Transient peak	After 30 min
$[Na^+]_e = 0$ ($n = 7$)	2.74±0.68	18.49±3.0	4.4±1.16
$[K^+]_e = 144$ mM ($n = 3$)	3.2±1.1	33.0±7.3	8.2±0.4
Verapamil (10^{-6} M) ($n = 5$)	4.4±0.6	Not measured	4.4±0.4

shown to abolish SR-dependent Ca^{++} oscillations in cardiac cells (Fabiato and Fabiato, 1973, 1975*b*; Dani et al., 1979). We therefore investigated the effect of caffeine on SLIF and the random diastolic contractile motion. Fig. 11*A* shows the variation of $f_{1/2}$ and correlation amplitude with increasing concentrations of caffeine in several muscles. The exact shape of the curves varied with the muscle and the ambient $[Ca^{++}]$. In some muscles there was a small increase in $f_{1/2}$ at low concentrations of caffeine; in all muscles the fluctuations were eventually abolished (flat autocorrelation function) at levels of caffeine of 10 mM or higher. Removal of caffeine resulted in a reappearance of SLIF. Many muscles show the behavior shown in the first three panels of the figure, in which $f_{1/2}$ falls to a plateau value around 1 Hz, and, beyond this point, amplitude decreases until fluctuations are undetectable (at which point, by convention, $f_{1/2} = 0$). In some muscles, there was a steady decline in $f_{1/2}$ with little fall in amplitude, as seen in the muscle in the fourth panel. As discussed in the Appendix, the former type of behavior would be expected if caffeine reduced the amplitude of the diastolic random motion without lowering its fundamen-

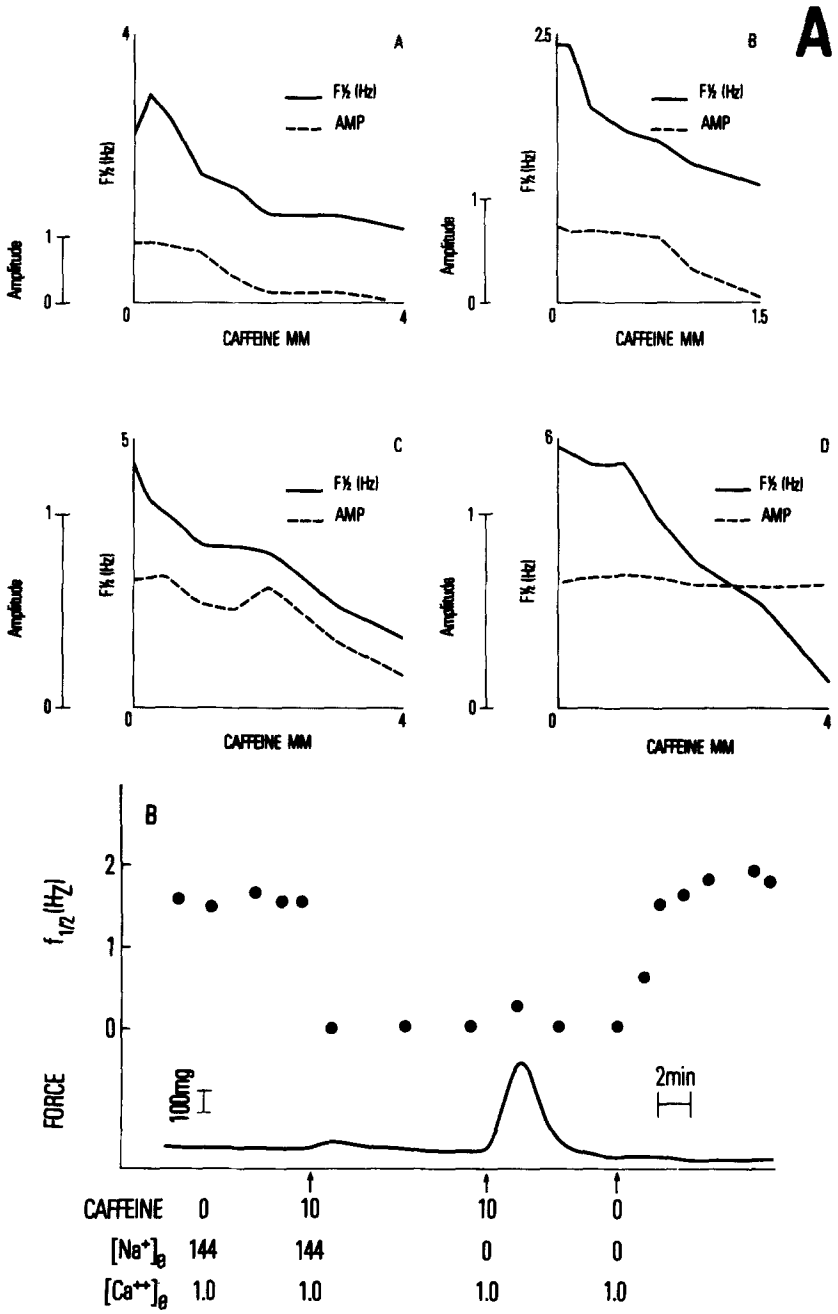

FIGURE 11. (*A*) Variation of $f_{1/2}$ and autocorrelation amplitude of light scattered at 30° from four (*A–D*) papillary muscles in $[Ca^{++}]_e$ = 2 mM as increasing concentrations of caffeine are added to the bath. Each panel represents one muscle. (*B*) Reduction of $f_{1/2}$ (dots) to zero by caffeine even in the presence of zero Na^+ contracture (cf. Fig. 10*A*). The slight rise of $f_{1/2}$ at the contraction peak is probably due to bulk-motion artifact.

tal frequency, whereas the latter indicates the occurrence of very low frequency intensity variation of significant amplitude even in the presence of caffeine. Rough calculation shows that a steady deformation of the muscle by as little as 1%/h would account for these variations, given the long averaging times used; therefore, the occurrence of the second type of behavior may well be an artifact of unsteady resting tension or stress relaxation of damaged ends. Fig. 11*B* shows the effect of removing Na^+ (replaced by Li^+) in the Krebs solution in the presence of 10 mM caffeine. The $f_{1/2}$ increase that usually accompanies the removal of Na^+ in the perfusate (Fig. 10*A*) has been blocked by caffeine.

When caffeine (10 mM) was applied to muscles in the microscope chamber, the diastolic random motion ceased completely within <1 min. Under coherent illumination, a stationary speckle pattern was seen in the presence of caffeine. When caffeine was removed, the motion of the muscle seen under incoherent light and the motion of the speckle pattern under coherent light gradually redeveloped in parallel over a period of ~5–8 min.

MODELS OF SLIF

The results above indicate that SLIF are closely correlated with the presence of random cellular motion within the muscle. Although it is not possible to exclude the presence of some refractive index fluctuations, it can be concluded that these are not present except in conditions when the motion is also present and thus would be difficult to detect by coherent optical methods in the presence of multiple scattering.

Fabiato and Fabiato (1975*b*, 1978*a*) and Fabiato (1981) have described mechanical oscillations in mechanically skinned cardiac myocytes with intact SR, subjected to partial EGTA buffering. By a carefully reasoned series of experiments they showed that mechanical oscillations are due to phasic oscillations of Ca^{++} surrounding the myofilaments caused by regenerative Ca^{++}-induced Ca^{++} release from the SR. Among the properties of these oscillations are the facts that their frequency and mechanical amplitude increase with the ambient pCa, that their amplitude is decreased by caffeine in the millimolar range (with an increase or no change in their frequency), and that they are abolished by removing ambient Ca^{++}, by applying 20 mM caffeine, or by exposure to Triton X-100, which destroys the SR. If we hypothesize that the diastolic random motion that we see in intact papillary muscles behaves in the same way with Ca^{++} and caffeine as do the mechanical oscillations seen by Fabiato (1981), the qualitative features of SLIF frequency and amplitude can be explained by the model system analyzed in the Appendix.

FORCE PRODUCTION BY RANDOM DIASTOLIC MOTION

Contraction of myofilaments anywhere within the muscle will always result in a small positive contribution to muscle tension, compared with the value when all myofilaments are relaxed. Therefore, in the presence of

random diastolic motion, there should be a net positive active tension that is the sum of all the contributions from different waves of contraction throughout the muscle. For a macroscopic muscle, the phasic components of tension from different parts of the muscle will largely cancel because they are asynchronous, resulting in an apparently steady Ca^{++}-dependent component of resting force. Since $f_{1/2}$ depends approximately on the average velocity of points in the tissue (not the wave velocity of contractile waves [see Appendix]), it is not surprising that it would correlate highly with average Ca^{++}-dependent resting force, especially when the variations of $f_{1/2}$ are largely due to variations in mechanical amplitude of the motion (see Appendix). The presence of diastolic random motion therefore provides an explanation of the Ca^{++}-dependent resting force observed previously (Lakatta and Lappe, 1981).

To analyze the role of Ca^{++}-dependent random motion in force production in diastolic muscle in more detail, it is necessary to model the motion. For this purpose we will make the naive assumption that the muscle is as an array of discrete "cells," each of which independently executes periodic contractions of the kind described by Fabiato and Fabiato (1975*b*) in isolated skinned cells. Individual cells will contract independently, and because their periods will differ from the mean, after a stimulated contraction they will get out of step within a few cycles and be completely asynchronous in the resting state. The displacements generated by one oscillator will spread passively through the macroscopic tissue along a three-dimensional network of series and parallel elastances; therefore, the effect of one cell will die away at distances that are large compared with a cell diameter. The displacement of an arbitrary tissue point in the midst of a macroscopic muscle will therefore be influenced only by oscillators in its own neighborhood and will be unaffected by distant oscillations and distant boundaries. Fig. 12*A* shows schematically how the motion of one point can be generated as the sum of displacements caused by the asynchronous oscillators in its neighborhood. The autocorrelation function of the motion can be calculated as the sum of the autocorrelation functions of the contributing oscillators; the latter are all positive periodic wave trains synchronized at $\Delta t = 0$ and they add up to produce the characteristic train of decaying peaks expected for the autocorrelation function of a partially periodic process, as shown in Fig. 12*B*. This is the motion autocorrelation function that is used in the Appendix as "$g(\Delta t)$" in analyzing the light-scattering problem; the qualitative features of that analysis do not depend on the details of the model from which it was obtained, but only on the presence of random partially periodic motion.

The force measured at the ends of the muscle will be the sum of the positive periodic wave trains produced by all the cells in the muscle. If there is a very large number of cells, there will be a steady component equal to $N\bar{f}$, where N is the number of cellular oscillators in the muscle and $\bar{f}$ is the mean force produced at the ends of the muscle by the

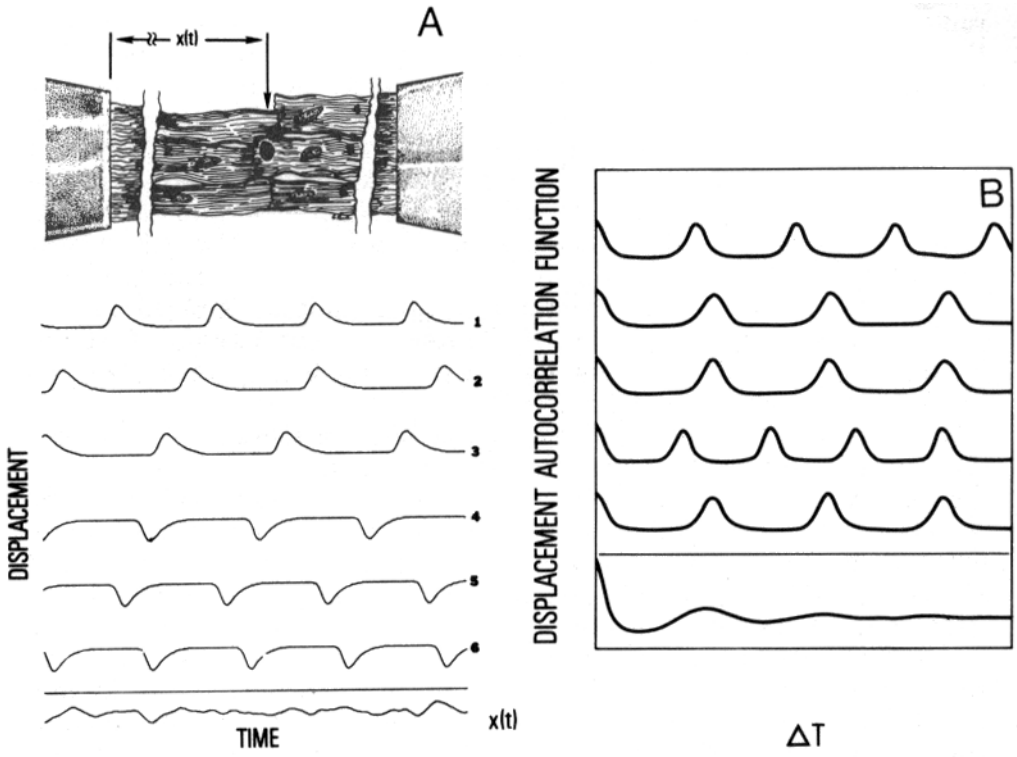

FIGURE 12. (*A*) Schematic of the model of independent cellular oscillators. The periodic asynchronous contractions of cells 1–6 contribute independently to the displacement of the scatterer in their neighborhood. The sum of their contributions is the randomly fluctuating displacement $x(t)$, which, despite its appearance, still has a partial periodicity that can be revealed by autocorrelation or spectrum analysis. The curve shown as $x(t)$ was computer-simulated by adding up 100 curves similar to curves 1–6 but with arbitrary phases and periods normally distributed about an average value. (*B*) The autocorrelation function of the motion $x(t)$ can be calculated as the sum of the autocorrelation functions for each of the oscillators. Since the latter are all positive periodic wave trains with the same phase (because each oscillator must be perfectly correlated with itself at $\Delta t = 0$ regardless of its absolute phase), the result is a series of diminishing peaks separated by intervals at Δt equal to the average oscillator period. The curve at the bottom was obtained by summing the 100 wave trains similar to the five at top. It is the curve used as $g(\Delta t)$ in the light-scattering calculation in the Appendix.

oscillation of one cell. The fluctuating component of force would be $f_{rms}\sqrt{N}$, where f_{rms} is the root-mean-square fluctuating component of force due to one oscillator. Clearly, in a muscle composed of thousands of cellular oscillators the steady force will predominate. Suppose, however, that all the oscillators could be synchronized at one point in time. Then the net force would consist of a summation of wave trains becoming

progressively out of phase with time, exactly analogous to the sum in Fig. 12*B*. This has been modeled for the case of an infinite number of oscillators whose intrinsic periods are distributed with a probability density $P(T)$. If $f(t)$ describes the periodic force produced by one oscillator with unit period, then the total force at time t after synchronization will be

$$F(t) = \int_0^\infty P(t)\, f(t/T)\, dT. \tag{1}$$

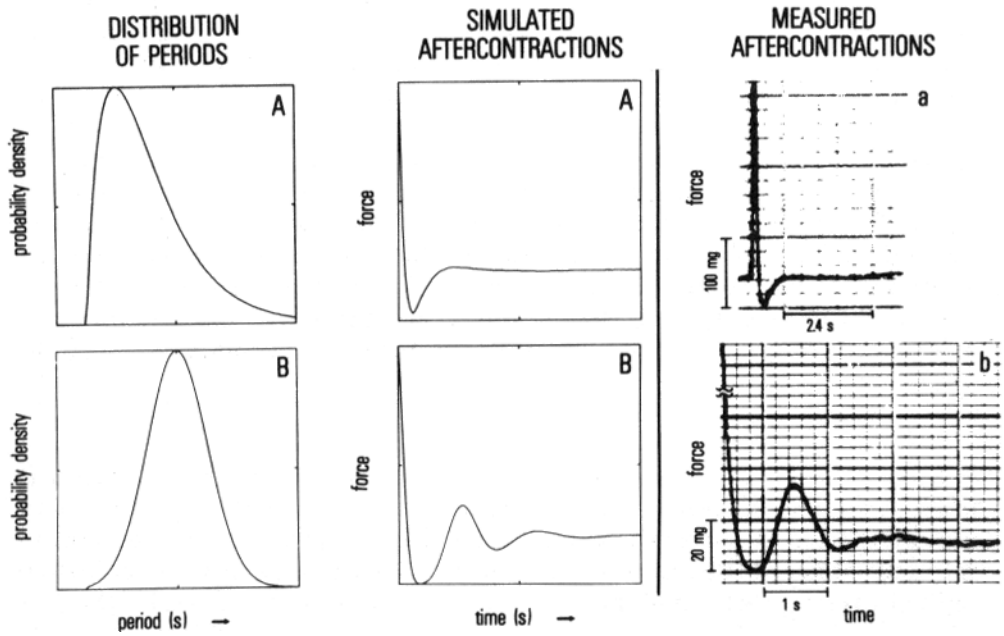

FIGURE 13. Simulated force transients produced by the synchronization model Eq. 1. The middle panels show force transients obtained by numerical integration of Eq. 1 using the probability distributions shown in the first panels as $P(T)$ and the periodic oscillation train $f(t)$, which was used in Fig. 12. The right-hand panels show actual aftercontractions measured from rat papillary muscles, selected for similarity to the calculated force transients. In row *A*, a skewed distribution of oscillation periods $[P(t) = (T - T0)e^{-aT}]$ gives rise to a force transient with a prominent hyper-relaxation and a subtle nonperiodic aftercontraction, resembling the measured transient (*a*) from a rat papillary muscle recently mounted in $[Ca^{++}]$ 1 mM. In row *B* a symmetrical (Gaussian) distribution of periods gives rise to a periodic series of aftercontractions, resembling the measured aftercontractions (*b*) from a muscle in $[Ca^{++}]_e$ = 2.5 and 2.5 mM caffeine.

In Fig. 13 are shown force transients generated by numerical integration of Eq. 1 using two alternative distributions of oscillator periods, one a symmetrical normal distribution, and the other a skewed distribution. The predicted force shows an initial large peak at the moment of synchronization, followed by a "hyper-relaxation," which occurs when all oscillators are simultaneously in their relaxed phase. There is then a series

of damped oscillations which are most conspicuous when the oscillators have a narrow, symmetric distribution of periods. Finally, force decays to the steady average level, which differs from the "hyper-relaxed" force by the amount of the "Ca^{++}-dependent resting force" $N\bar{f}$. Hyper-relaxation and aftercontractions following the twitch are well-described phenomena in rat cardiac muscle in physiological $[Ca^{++}]_e$ (Posner and Berman, 1969) and in other species under conditions of high Ca^{++} loading (Bozler, 1943; Reiter, 1962; Katzung, 1964; Braveny et al., 1966; Ferrier, 1976). Actual aftercontractions recorded from rat papillary muscles under different conditions of Ca^{++} loading are shown in the third panel of Fig. 13 for comparison with the calculated force transients. Obviously, this is not intended to imply that the naive oscillator model provides a quantitative explanation of these phenomena, but merely that synchronization of ongoing oscillations is one plausible mechanism by which aftercontractions might be generated. Direct microscopy of muscles during stimulation showed that diastolic random motion and the corresponding laser speckle motion do in fact cease during the hyper-relaxation immediately after the twitch and then redevelop during the aftercontraction, but whether the motions are "synchronized" or reappear in fully asynchronous form could not be decided by visual inspection.

DISCUSSION

We have found by incoherent light microscopy that tissue motion is present on a scale more than sufficient to produce SLIF, and that SLIF are detected in precisely those states in which the diastolic random motion is found. Many of the physical characteristics of SLIF measured via formal light-scattering techniques are compatible with a model in which there is widespread asynchronous motion whose mechanical amplitude is increased by Ca^{++} and decreased by caffeine and whose frequency may increase with Ca^{++}. The scattering angle dependencies of $f_{1/2}$ and intensity autocorrelation amplitude are not compatible with first-order scattering from such a model, but because these muscles are optically thick, deep-phase screen effects and multiple scattering could produce the kind of angle dependence observed even when the underlying process is longitudinal motion (Haskell and Carlson, 1981). In addition, fluctuating deep-phase effects are likely to be present because of variation in the thickness of the muscle caused by the waves of cellular motion as observed by direct microscopy. Accordingly, our data neither require nor suggest the presence of refractive index fluctuations, and they indicate that such fluctuations could only be present concurrently with motion.

Asynchronous motion of the kind we describe has been observed previously in cardiac muscle during Na^+-free contracture (Anderson et al., 1976). Our studies show that similar but more subtle motion also occurs under more physiologic conditions and is easily detected by coherent light scattering. It is unlikely that motions coherent over many microns and involving displacements up to tens of microns could be generated by

any mechanism other than the myofilaments. The fact that steady activation of myofilaments by constant, buffered levels of myoplasmic [Ca^{++}] does not produce either observable motions or SLIF, and that both are suppressed in caffeine, shows that myofilament activation per se does not generate these fluctuations. This excludes, for example, fluctuations caused by asynchronous cycling of cross-bridges at the sarcomere level (Carlson, 1975; Borjedo and Morales, 1977). The relationship of SLIF in rat heart muscle to those studied in skeletal muscle by Bonner and Carlson (1975) and Haskell and Carlson (1981) is conjectural. The latter occur during maximal tetanic activation, in which a steady state of myofilament activation is usually assumed. The motions that we have observed in cardiac muscle occur in the absence of stimulation and appear to be somewhat larger than those in skeletal muscle. The "myogenic" sarcomere oscillations observed by Fabiato and Fabiato (1978*b*) also are probably not the cause of SLIF, since they should not be abolished in skinned myofilaments.

Our results imply that in nonstimulated rat cardiac muscle, Ca^{++} activating the myofilaments fluctuates in time and space, thereby driving the myofilaments to produce the diastolic random motion. It is noteworthy that earlier studies (Lappe and Lakatta, 1980) showed the presence of vigorous SLIF when Ca^{++} was replaced in the perfusate in muscles rendered hyperpermeable by EDTA. The fact that the "EDTA-skinned" muscles did not exhibit the steep force-pCa curves found in detergent-skinned muscles in the present study, and that they did exhibit SLIF, suggests that in this preparation the SR is intact and that myoplasmic [Ca^{++}] is incompletely buffered (Miller, 1979).

The present results permit the inference that there are fluctuations of myoplasmic [Ca^{++}] in "resting" rat heart muscle, and that these fluctuations cause diastolic random motion, which is the principle cause of SLIF. What produces the Ca^{++} fluctuation? The fact that they are not abolished in the absence of Na^{+}, in the presence of verapamil, or during sarcolemmal depolarization indicates that electrical oscillations at the sarcolemma are not required. Their behavior with caffeine and with variation of $[Ca^{++}]_i$ suggests that the SR is involved in their production. In fact, this behavior is closely analogous to the behavior of oscillations in mechanically skinned cardiac cells caused by Ca^{++}-induced Ca^{++} release that have been observed in disaggregated mouse, rat, and rabbit ventricular cells (Bloom et al., 1974; Fabiato and Fabiato, 1975*b*; Fabiato, 1981), cultured cardiac myocytes (Goshima, 1976), and disrupted rabbit ventricular cells (Dani et al., 1979).

Glitsch and Pott (1975) observed minute spontaneous fluctuations in resting tension of small guinea pig atrial trabeculae in states of high Ca^{++} loading; these were decreased in amplitude and then suppressed by millimolar concentrations of caffeine, but were not blocked by slow channel blockade with Mn^{+} or depolarization with KCl. Similarly, spontaneous voltage fluctuations induced by Ca^{++} overload due to cardiac

glycosides have been measured in single guinea pig ventricular cells (Matsuda et al., 1982). These oscillations were abolished by intracellular EGTA and decreased in amplitude with caffeine. The principle distinction between these spontaneous oscillations in guinea pig trabeculae and cells and the SLIF observed in rat papillary muscles is that the latter can be detected in intact muscles under "normal" conditions of Ca^{++} loading. Possible reasons for this include both a species difference and the great sensitivity of the laser scattering method to detect motion that is at the limit of resolution of light microscopy. If SLIF are in fact due to Ca^{++}-induced Ca^{++} release, then the present results indicate that this process occurs under "physiologic" conditions in intact rat myocardium. The presence of diastolic SLIF has also been documented in several types of cardiac tissue from a range of species. The experimental conditions required for SLIF to be present in the steady state vary with a given species. Frog myocardium, however, does not exhibit SLIF even under conditions that result in marked cellular Ca^{++} overload (Lakatta and Lappe, 1981; Kort and Lakatta, 1981). This pronounced species variation in similarly mounted preparations of equal average thickness indicates that SLIF cannot simply be attributed to damage sustained at the ends of the tissue in mounting (Vassallo and Pollack, 1982).

The occurrence of diastolic random motion in "resting" rat ventricular muscle provides an explanation, in part at least, of the phenomenon of Ca^{++}-dependent resting force in non-Ca^{++}-overloaded muscles that was otherwise somewhat puzzling because free myoplasmic [Ca^{++}] is usually thought to fall below the level required for activation of the myofilaments during diastole. It is important to note, however, that under some experimental conditions, i.e., those that result in high cellular Ca^{++} loading or when caffeine is present, "resting" force can exhibit a tonic Ca^{++}-dependent component. When mechanical oscillations are present, the waves of contraction are asynchronous and the mechanical loading conditions seen by the activated myofilaments will not be isometric; therefore, the random diastolic motion may do more work than the average level of Ca^{++}-dependent diastolic force would suggest. This may account for the very high resting heat production found in rat myocardium (Loiselle and Gibbs, 1979).

As shown in our "naive model" calculations, if the diastolic motion is due to synchronizable periodic oscillators, this might provide an explanation of the transients of diastolic force that are produced after a beat. Even if this is the case, the calculation cannot be used to predict aftercontractions quantitatively because it ignores the fact that the oscillations involve traveling waves (both in intact muscle and isolated cells) and that total cellular Ca^{++} loading may undergo its own transient variations after Ca^{++} fluxes across the sarcolemma during the action potential.

Aftercontractions have been observed in association with periodic transient inward currents following voltage steps in Purkinje fibers treated with cardiac glycosides (Ferrier et al., 1973; Ferrier, 1976; Lederer and

Tsien, 1976; Kass et al., 1978*a*, *b*). Spontaneous fluctuations of membrane current have also been observed in these preparations (Lederer, 1976; Kass et al., 1976), which appear to have the same partially periodic spectrum (fundamental frequencies 1–2 Hz) as the transient inward current triggered by depolarization, as would be predicted if the latter were due to synchronization of an array of independent oscillators. By studying the effects of membrane potential, Ca^{++} blockers, and ionic manipulation, Lederer and Tsien (1976) and Kass et al. (1978*b*) also concluded that the primary event underlying these membrane currents is an oscillatory release of Ca^{++} from intracellular stores. Preliminary studies in Purkinje fibers (Kort and Lakatta, 1981) indicate that this tissue exhibits diastolic SLIF even in the absence of Ca^{++} overload, and that glycosides and other forms of cellular Ca^{++} loading increase $f_{1/4}$ and caffeine abolishes $f_{1/2}$ in a fashion similar to that in rat ventricular myocardium. This suggests that cellular Ca^{++} oscillations in Purkinje fibers occur even in the absence of Ca^{++} overloading and that laser spectroscopy can be used to assess these oscillations without employing depolarizing voltage steps.

A most important conclusion derived from the present studies is that at a given inotropic state, myoplasmic $[Ca^{++}]$ is probably not in a microscopic steady or homogeneous state during diastole. Furthermore, the magnitude and frequency of myoplasmic $[Ca^{++}]$ oscillations manifest as changes in SLIF vary directly with the inotropic state in rat ventricular muscle (Lakatta and Lappe, 1981), which suggests a possible role in excitation-counteraction coupling. Finally, steady state concepts such as diastolic compliance, compartmental Ca^{++} pools, or resting sarcomere length must be evaluated with caution in heart muscle.

APPENDIX

If, in fact, the tissue motion is entirely responsible for SLIF, it should be possible to calculate the fluctuation spectrum from the motion. Unfortunately, even if we possessed a complete statistical characterization of the diastolic motion (i.e., the complete space-time autocorrelation moments of the displacement to all orders), the calculation of the scattered-light spectrum in the presence of deep-phase screen and multiple scattering effects would be formidable. However, a descriptive characterization of the motion does permit examination of an over-simplified model system in which first-order scattering occurs from a random array of light scatterers located throughout the muscle, which are fixed as to their mean positions, but undergo independent fluctuating displacements about these means.

Let the longitudinal position of the jth scatterer be $X_j = x_j + y_j(t)$, where x_j are independent random variables characterizing the mean positions of the scatterers and $y_j(t)$ are independent stochastic processes describing the motion of the scatterers about their mean positions. In reality, individual light-scattering structures in the muscle will not have independent motions if they are within a few microns of one another, but microscopy indicates that the 1-mm illumination area should contain a large number of independently moving regions. The complex electromagnetic field amplitude (horizontally polarized) will be a super-

position

$$E(t) = \sum_j a_j e^{ik[x_j + y_j(t)]}, \tag{2}$$

where a_j is the scattering amplitude of the jth scatterer and $k \equiv 2\pi \sin \theta/\lambda$ is defined in terms of the scattering angle θ and the wavelength λ of light. The field autocorrelation function of the scattered light is

$$G(t_1 - t_2) \equiv \langle E(t_1)E^*(t_2)\rangle = \sum_{j,l} a_j^* a_l \langle e^{ik(x_j - x_l)} e^{ik[y_j(t_1) - y_l(t_2)]}\rangle. \tag{3}$$

Since the illuminated area through which x_j are distributed is much larger than a wavelength of light, only terms for which $j = l$ will have significant expectation values, so that

$$G(t_1 - t_2) = \sum_j |a_j|^2 \langle e^{ik[y_j(t_1) - y_j(t_2)]}\rangle = I\langle e^{ik[y(t_1) - y(t_2)]}\rangle, \tag{4}$$

where I is the mean intensity of scattered light and we have removed the subscripts for the y's in the exponential because the motions of all scatterers are assumed to be statistically similar. To facilitate calculation in this idealized model we will assume that the random motions $y(t)$ are Gaussian processes, as would be the case if the displacement of a scatterer were the result of superposition of numerous independent random forces from cells in its neighborhood. Then the expectation value in the last line of Eq. 4 can be calculated to be (Saleh, 1978)

$$G(\Delta t) = Ie^{-\sigma^2 k^2[1 - g(\Delta t)]} \tag{5}$$

where $\sigma^2 \equiv \text{var}(y) = \langle y_i^2\rangle$ and $g(\Delta t) \equiv \langle y_i(t_1)y(t_2)\rangle/\sigma^2$ is the normalized autocorrelation function of the motion of the typical scatterer. The function $g(\Delta t)$ embodies the time-varying behavior of the random motion, and σ is the rms displacement of the scatterer by the motion.

The quantity actually measured in intensity fluctuation spectroscopy is the autocorrelation function of the intensity $I(t) \equiv |E(t)|^2$. If the number of scatterers is large, the field will have Gaussian statistics, and it can be shown (cf. Saleh, 1978) that the intensity autocorrelation function is

$$G^{(2)}(\Delta t) = I^2 + G^2(\Delta t) = I^2\{1 + e^{-2\sigma^2 k^2[1 - g(\Delta t)]}\}, \tag{6}$$

which expresses the experimentally measured function in terms of the hypothetical correlation function of the motion $g(\Delta t)$ and the mechanical amplitude of the motion σ.

The autocorrelation function of the motion $g(\Delta t)$ for a "partially periodic" random motion will be a decaying series of peaks separated by intervals equal to the average fundamental period of the motion. The lower curve in Fig. A1 is an example of such a function; in this case it was derived from a model of the motion as a superposition of discrete oscillators, as discussed in the text. The upper two curves show the intensity autocorrelation function calculated from Eq. 6 using the lower curve for $g(\Delta t)$ and assuming two different values (142 and 285 nm) for the mechanical amplitude σ. For the smaller mechanical amplitude the shape of the intensity correlation function mimics that of the motion correlation function. As the mechanical amplitude of the motion increases relative to the wavelength of light, several changes occur, as shown in the figure. The first

is that the steepness of decay of the first (principal) autocorrelation peak, which determines $f_{1/2}$, increases. The second is that the relative height of the secondary autocorrelation peaks decreases. If the second peak of $g(\Delta t)$ is less than the first by an amount a, the second peak of the intensity correlation will be reduced (compared with the principle peak) by a factor $e^{-2k^2\sigma^2 a}$, which decreases rapidly with σ. When the mechanical amplitude becomes larger than the wavelength of light the second and later peaks are reduced to the point of undetectability. The third change is an increase of intensity correlation amplitude as mechanical amplitude increases, as discussed below.

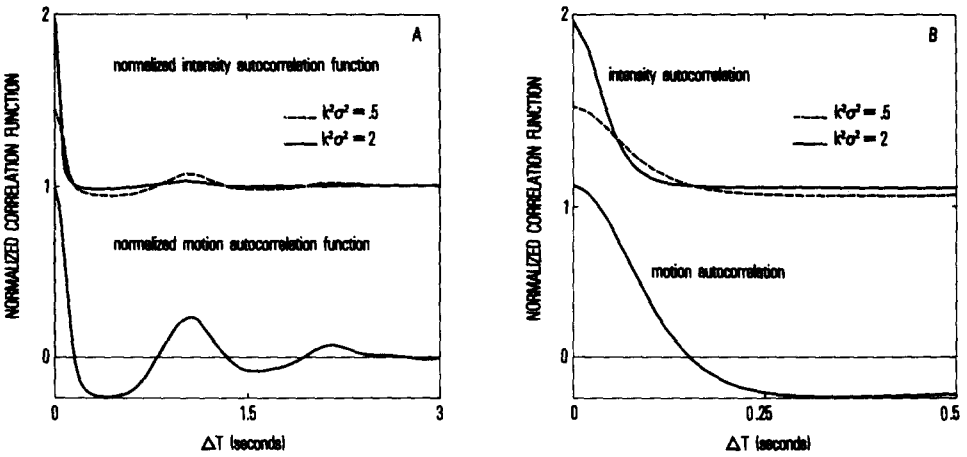

FIGURE A1. Motion autocorrelation function of a partially periodic random point displacement (lower curve) and the scattered-light intensity correlation functions calculated from it by Eq. 6 (upper curves) for two values of the rms displacement parameter $k\sigma$. For scattering of He-Ne laser light at an angle of 30°, this corresponds to rms scatterer displacements of 142 (dashed curve) and 285 nm (upper solid curve). The increased steepness of decay of the primary peak and the suppression of the secondary peaks as $k\sigma$ increases are shown. The motion autocorrelation function shown was derived from the model of independent cellular oscillators described in the text. The right-hand panel is an expanded timebase showing the portion of the intensity autocorrelation function actually used in computing $f_{1/2}$.

If we hypothesize that the diastolic random motion we see in intact papillary muscles behaves in the same way with Ca^{++} and caffeine as do the mechanical oscillations seen by Fabiato (1981), the qualitative features of SLIF frequency and amplitude can be explained by the model. In the presence of large motions visible by incoherent light microscopy, $\sigma k > 1$ and the light-intensity correlation amplitude would be expected to be maximal and $f_{1/2}$ to be increased by raising Ca^{++} [which increases both σ and the dominant frequencies of $g(\Delta t)$] and to be decreased by caffeine, which lowers σ. When the motion is large, theory predicts that the secondary autocorrelation peaks indicative of periodicity of the motion will not appear in the light-intensity autocorrelation functions. When Ca^{++} is lowered or caffeine is raised sufficiently to reduce σ below $\lambda/2\pi$, the intensity

autocorrelation amplitude would be expected to decline steeply. The behavior of $f_{1/2}$ under these conditions depends on how the underlying motion frequencies are affected. If the motion frequencies fall (as might be expected in low-Ca^{++} states) then $f_{1/2}$ should fall smoothly to zero. If the mechanical spectrum remains the same while the amplitude of the motion declines (as may be the case with caffeine), then $f_{1/2}$ will decline with σ until $\sigma k \cong 1$, beyond which $f_{1/2}$ will plateau while intensity autocorrelation amplitude declines to zero (see below). It should be noted that when the amplitude is very low, measurement of $f_{1/2}$ becomes difficult; in particular, any secular deformation of the illuminated segment of the muscle by as much as a wavelength of light during the several minutes over which the autocorrelation function is averaged (e.g., stress relaxation of the damaged ends of the muscle) will result in spuriously high values of amplitude, leading to correspondingly low estimates of $f_{1/2}$ from the autocorrelation function.

Under conditions in which $\sigma k \leq 1$, when a secondary peak is present in the motion autocorrelation function, a secondary peak in the intensity autocorrelation function is also exhibited, as shown in Fig. A1. The oscillations described by Fabiato and Fabiato (1975*a*) are highly periodic; the random diastolic motion of intact muscle shows a less conspicuous but definite local periodicity. We therefore sought evidence of periodicity by measuring autocorrelation functions on a long timebase in muscles in concentrations of caffeine that reduced $f_{1/2}$ and lowered correlation amplitude but less than that which abolishes fluctuations entirely. Fig. A2 shows such an autocorrelation function from the same muscle shown (in the absence of caffeine) in Fig. 8. In caffeine, there is now a late peak corresponding to a periodic component with a period of 410 ms. Peaks at 400–2,000 ms were observed regularly under these conditions; they are abolished at higher levels of caffeine when amplitude and $f_{1/2}$ go to zero. As shown in the figure, the location of the late peak is independent of scattering angle, excluding the possibility that it is due to a Doppler frequency caused by steady motion of part of the muscle. In any case, steady motion at the speed required over the 15-min averaging period would result in a net translation >1 mm. We therefore believe these peaks are evidence of underlying periodicity of the process in the muscle.

Calculation of the intensity correlation amplitude requires us to consider a point of some subtlety. When the motion of the scatterers is less than the wavelength of light, the scattered light intensity will not be time-ergodic, because the time-mean intensity at one point in the scattering pattern will depend on the particular values of the "random" mean positions x_j, of which only one realization is included in any one time average. The physical meaning of this is that for small values of σ, there will be a stationary speckle pattern superimposed on the fluctuating light, and the value of the amplitude will vary depending on whether the detector is located on a bright or dark speckle of this pattern. There are two ways to define the "average" amplitude. One would be to measure the intensity autocorrelation function on an ensemble of muscles (or, more reasonably, at a number of different coherence areas in the neighborhood of the same scattering angle in one muscle), average these correlation functions, normalize the result, and compute the amplitude from it. This is essentially what was done in the above calculation. To determine the amplitude, $G^2(\Delta t)$ should be normalized by its asymptotic value at $\Delta t \to \infty$, which gives

$$A_{\text{ensemble}} = \frac{1 - e^{-2k^2\sigma^2}}{1 + e^{-2k^2\sigma^2}} . \tag{7}$$

The second approach, which corresponds more closely to the way the data are actually handled, is to compute the intensity autocorrelation function at one point for one muscle as a time average, normalize it and compute the amplitude, and then average the result over the random positions x_j. If x_j are treated as fixed, the field at one point in the scattering pattern may be resolved into the sum of circular Gaussian light and constant elastically scattered coherent light, the intensity of the latter varying from one point to another in the stationary speckle pattern. The autocorrelation amplitude can be computed, in a tedious

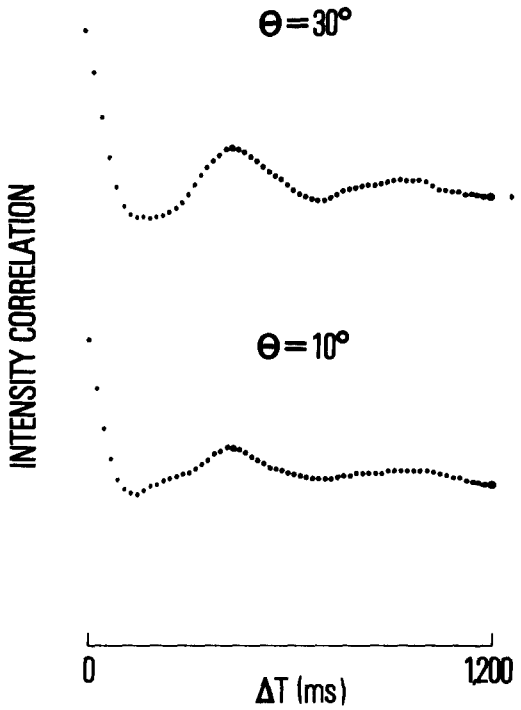

FIGURE A2. Long timebase autocorrelation function of light scattered by a papillary muscle in $[Ca^{++}] = 2$ mM and 2 mM caffeine, at scattering angles of 30° (upper panel) and 10° (lower panel). This is the same muscle whose long timebase autocorrelation function was shown in Fig. 8 in the absence of caffeine. Note the presence of secondary autocorrelation peaks in the presence of caffeine and the fact that the position of the secondary peak is independent of angle, which indicates that it is caused by a periodic process in the muscle rather than a Doppler shift caused by steady motion.

but straightforward manner, and then averaged over the ensemble of possible values of x_j. The result is

$$A_{\text{point average}} = \int_0^\infty \frac{1 + 2y/(e^{k^2\sigma^2} - 1)}{[1 + y/(e^{k^2\sigma^2} - 1)]^2} dy. \tag{8}$$

The amplitude calculated in these two ways is plotted as a function of σ in Fig. A3 for the case of 30° scattering of He-Ne light. Both calculations show similar behavior: for motion large compared with the wavelength, the amplitude is unity,

corresponding to Gaussian statistics. When the motion becomes smaller than the wavelength, there is a rapid decline of A until is approaches zero when the motion is undetectable by visible light.

When the amplitude is small (mechanically and optically), the shape of the autocorrelation function of the light becomes the same as that of the underlying motion. In this case, $f_{1/2}$ approaches a plateau value (as a function of σ), which is determined by the frequencies of the underlying mechanical motion. If σ becomes large, on the other hand, the intensity autocorrelation function tends toward a Gaussian shape regardless of the details of $g(\Delta t)$; in this case, the light spectrum is a Doppler spectrum related to the distribution of instantaneous velocities of scatterers. The rms velocity of scatterers is found to be (for the case

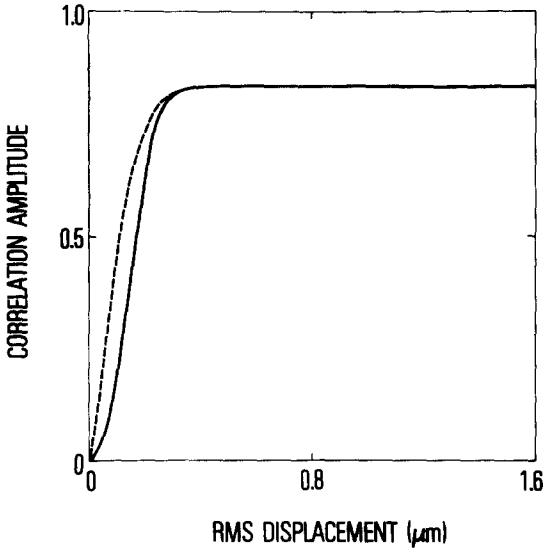

FIGURE A3. Average correlation amplitude calculated from Eq. 7 (solid curve) or Eq. 8 (dashed curve) as a function of scatterer rms displacement for the model of He-Ne laser light scattered at 30° from an array of independent scatterers undergoing random constrained motions about their mean positions. The shape of the curves is independent of the details of the motion autocorrelation function.

of first-order scattering)

$$V_{\text{rms}} = l f_{1/2}; \qquad l = 0.37\ \mu\text{m}, \tag{9}$$

where V_{rms} is in micrometers per second and $f_{1/2}$ is in hertz. These velocities appear to be well within the range estimated by incoherent microscopy.

Received for publication 7 June 1982 and in revised form 11 February 1983.

REFERENCES

Anderson, P. A. W., A. Manring, J. R. Sommer, and E. A. Johnson. 1976. Cardiac muscle: an attempt to relate structure to function. *J. Mol. Cell. Cardiol.* 8:123–143.

Blayney, L., H. Thomas, J. Muir, and A. Henderson. 1978. Action of caffeine on calcium transport by isolated fractions of myofibrils, mitochondria, and sarcoplasmic reticulum from rabbit heart. *Circ. Res.* 43:520–526.

Bloom, S., A. J. Brady, and G. A. Langer. 1974. Calcium metabolism and active tension in mechanically disaggregated heart muscle. *J. Mol. Cell. Cardiol.* 8:137–147.

Bonner, R. F., and F. D. Carlson. 1975. Structural dynamics of frog muscle during isometric contraction. *J. Gen. Physiol.* 65:555–581.

Borejdo, J., and M. F. Morales. 1977. Fluctuations in tension during contraction of single muscle fibers. *Biophys. J.* 20:315–334.

Bozler, E. 1943. Tonus changes in cardiac muscle and their significance for the initiation of impulses. *Am. J. Physiol.* 139:477–480.

Braveny, P., J. Sumbera, and V. Kruta. 1966. After contractions and restitution of contractility in the isolated guinea-pig auricles. *Arch. Int. Physiol.* 74:169–178.

Carlson, F. D. 1975. Structural fluctuations in the steady state of muscular contraction. *Biophys. J.* 15:633–649.

Dani, A. M., A. Cittadini, and G. Inesi. 1979. Calcium transport and contractile activity in dissociated mammalian heart cells. *Am. J. Physiol.* 237(3):C147–C155.

Endo, M. 1977. Calcium release from the sarcoplasmic reticulum. *Physiol. Rev.* 57:71–108.

Endo, M., and T. Kitazawa. 1978. E-C coupling in skinned cardiac fibers. *In* Biophysical Aspects of Cardiac Muscle. M. Morad, editor. Academic Press, Inc., New York. 307–327.

Fabiato, A. 1981. Myoplasmic free calcium concentration reached during the twitch of an intact isolated cardiac cell and during calcium-induced release of calcium from the sarcoplasmic reticulum of a skinned cardiac cell from the adult rat or rabbit ventricle. *J. Gen. Physiol.* 78:457–497.

Fabiato, A., and F. Fabiato. 1973. Activation of skinned cardiac cells. Subcellular effects of cardiovascular drugs. *Eur. J. Cardiol.* 1:143–155.

Fabiato, A., and F. Fabiato. 1975*a*. Effects of magnesium on contractile activation of skinned cardiac cells. *J. Physiol. (Lond.).* 249:497–517.

Fabiato, A., and F. Fabiato. 1975*b*. Contractions induced by a calcium-triggered release of calcium from the sarcoplasmic reticulum of single skinned cardiac cells. *J. Physiol. (Lond.).* 249:469–495.

Fabiato, A., and F. Fabiato. 1978*a*. Calcium-induced release of calcium from the sarcoplasmic reticulum of skinned cells from adult human, dog, cat, rabbit, rat, and frog hearts and from fetal and new-born rat ventricules. *Ann. NY Acad. Sci.* 307:491–522.

Fabiato, A., and F. Fabiato. 1978*b*. Myofilament-generated tension oscillations during partial calcium activation and activation dependence of the sarcomere length-tension relation of skinned cardiac cells. *J. Gen. Physiol.* 72:667–699.

Fabiato, A., and F. Fabiato. 1979. Calculator programs for computing the composition of the solutions containing multiple metals and ligands used for experiments in skinned muscle cells. *J. Physiol. (Paris).* 75:463–505.

Ferrier, G. R. 1976. The effects of tension on acetylstrophanthidin-induced transient depolarizations and aftercontractions in canine myocardial and Purkinje tissues. *Circ. Res.* 28:156–162.

Ferrier, G. R., J. H. Saunders, and C. Mendez. 1973. A cellular mechanism for the generation of ventricular arrhythmias by acetylstrophanthidin. *Circ. Res.* 32:600–609.

Glitsch, H. G., and L. Pott. 1975. Spontaneous tension oscillations in guinea-pig atrial trabeculae. *Pflügers Arch. Eur. J. Physiol.* 358:11–25.

Goshima, K. 1976. Arrhythmic movements of myocardial cells in culture and their improvement with antiarrhythmic drugs. *J. Mol. Cell. Cardiol.* 8:217–238.

Haskell, R. C., and F. D. Carlson. 1981. Quasi-elastic light-scattering studies of single skeletal muscle fibers. *Biophys. J.* 33:39–62.

Kass, R. S., W. J. Lederer, and R. W. Tsien. 1976. Current fluctuations in strophanthidin-treated cardiac Purkinje fibers. *Biophys. J.* 16:25*a*. (Abstr.)

Kass, R. S., W. J. Lederer, R. W. Tsien, and R. Weingart. 1978*a*. Role of calcium ions in transient inward currents and aftercontractions induced by strophanthidin in cardiac Purkinje fibres. *J. Physiol. (Lond.).* 281:187–208.

Kass, R. S., R. W. Tsien, and R. Weingart. 1978*b*. Ionic basis of transient inward current induced by strophanthidin in cardiac Purkinje fibres. *J. Physiol. (Lond.).* 281:209–226.

Katzung, F. 1964. Diastolic oscillation in muscle tension and length. *J. Cell. Comp. Physiol.* 64:103–114.

Kimoto, Y., M. Saito, and M. Goto. 1974. Effect of caffeine on the membrane potentials, membrane currents and contractile of the bullfrog atrium. *Jpn. J. Physiol.* 24:531–542.

Kort, A. A., and E. G. Lakatta. 1981. Light scattering identifies diastolic myoplasmic Ca^{2+} oscillation in diverse mammalian cardiac tissues. *Circulation.* 64:IV–162.

Lakatta, E. G., and D. L. Lappe. 1981. Diastolic scattered light fluctuation, resting force and twitch force in mammalian cardiac muscle. *J. Physiol. (Lond.).* 315:369–394.

Lappe, D. L., and E. G. Lakatta. 1980. Intensity fluctuation spectroscopy monitors contractile activation in "resting" cardiac muscle. *Science (Wash. DC).* 207:1369–1371.

Lederer, W. J. 1976. The ionic basis of arrhythmogenic effects of cardiotonic steroids in cardiac Purkinje fibers. Ph.D. Thesis, Yale University, New Haven, CT.

Lederer, W. J., and R. W. Tsien. 1976. Transient inward current underlying arrhythmogenic effects of cardiotonic steroids in Purkinje fibres. *J. Physiol. (Lond.).* 262:73–100.

Loiselle, D. S., and C. L. Gibbs. 1979. Species differences in cardiac energetics. *Am. J. Physiol.* 237(1):H90–H98.

McClellan, G. B., and S. Winegrad. 1978. The regulation of the calcium sensitivity of the contractile system in mammalian cardiac muscle. *J. Gen. Physiol.* 72:737–764.

Matsuda, H., A. Noma, Y. Kurachi, and H. Irisawa. 1982. Transient depolarization and spontaneous voltage fluctuations in isolated single cells from guinea pig ventricles. Calcium-mediated membrane potential fluctuations. *Circ. Res.* 51:142–151.

Miller, D. J. 1979. Are cardiac muscle cells 'skinned' by EGTA or EDTA? *Nature (Lond.).* 277:142–143.

Posner, C. J., and D. A. Berman. 1969. Mathematical analysis of oscillatory and non-oscillatory recovery of contractility after a rested-state contraction and its modification by calcium. *Circ. Res.* 25:725–733.

Reiter, M. 1962. Die Entstehung von "Nachkontraktionen" im Herzmuskel unter Einwirkung von Calcium und von Digitalisglykosiden in Abhangigkeit von der Reizfrequenz. *Naunyn-Schmiedeberg's Arch. Exp. Pathol. Pharmakol.* 242:497–507.

Reuben, J. P., and D. S. Wood. 1979. Matters arising: are cardiac muscle cells skinned by EGTA or EDTA? *Nature (Lond.).* 280:700–701.

Saleh, B. 1978. Photoelectron Statistics, with Application to Spectroscopy and Optical

Communication. Springer Series in Optical Science. Springer-Verlag, Berlin. 6:190–388.

Vassallo, and G. H. Pollack. 1982. The force-velocity relation and stepwise shortening in cardiac muscle. *Circ. Res.* 51:37–42.

Weber, A. 1968. The mechanism of the action of caffeine on the sarcoplasmic reticulum. *J. Gen. Physiol.* 52:760–772.